ISET Journal of Earthquake Technology, Paper No. 597, Vol. 62, No. 2, June 2025, pp. 113-127

NEXT-GENERATION EARTHQUAKE INTENSITY AND MAGNITUDE PREDICTION EQUATIONS FOR HIMALAYAN REGION

Anbazhagan P.*
Department of Civil Engineering, Indian Institute of Science
Bengaluru-560012, Email id: anbazhagan@iisc.ac.in

Harish Thakur
Department of Civil Engineering, Indian Institute of Science
Bengaluru-560012, Email id: harishthakur@iisc.ac.in

ABSTRACT

Intensity Prediction Equations (IPEs) are essential to produce seismic risk mapping, and a very limited number of such models are available for the Himalayan Region. This study presents macroseismic intensity-based relations – (i) magnitude (M_w) vs. maximum Intensity (I_{max}) equations for past earthquakes, (ii) IPEs for risk estimation and (iii) I_{max} vs M_w for future earthquakes. For the development of IPEs, two distinct intensity datasets were catalogued using macroseismic information from past studies: (a) considering published information from field studies and print media, and (b) using online questionnaires (like DYFI, an initiative by the USGS). In addition, the present study reevaluated the intensities of conventional datasets for a few earthquake events in various assignment scales homogenized to a common scale. A one-stage and two-stage regression technique is used to derive IPEs for both datasets. These IPEs are designed for a second-order relationship of seismic intensity w.r.t. event's Magnitude. Choosing the most appropriate IPEs using a maximum intensity versus magnitude approximation of the IPE's approach has also been suggested, which depends on an optimal hypocentral depth. The damage potential of upcoming earthquakes can be evaluated using these recently created equations.

KEYWORDS: Intensity Prediction Equations; Macroseismic Intensity, Magnitude-Intensity Relationships; Seismic Risk Assessment; EMS-98

INTRODUCTION

Seismic Intensity values are a pure representation of damage and human and economic losses due to seismic events. Historically, intensities were used to quantify the size of an earthquake qualitatively, as they are a function of observed damage. After developing a quantitative earthquake size scale of magnitudes, intensities are less commonly used to represent size because they are also a function of different seismic hazards, such as amplification, liquefaction, and the condition of buildings and population distribution in the region. Still, intensities are in greater demand as these are only earthquake information for the regions that do not have earthquake recording instruments or events before magnitude estimation. Intensities are widely used to assess damage and risk due to seismic hazards. Even Indian Seismic zonation maps at different periods were based on past earthquake intensities observed in the region rather than systematic hazard estimation (Anbazhagan et al., 2014). Seismic Zonation map in IS 1893 shows that Northern India is in Zones III and IV, with a few areas falling under Zone V. The entirety of North-East India is under Zone V, according to Indian code IS 1893 (Part 1): 2016 Seismic Zonation Map of India. According to the code, Intensities VII, VIII, and IX (and above) of the 1964 Medvedev-Sponheuer-Karnik scale, or MSK-64, correspond to Zones III, IV, and V. The most damaging intensities are marked as higher seismic zones of the Indian code, according to maximum shaking intensity maps created by Martin and Szeliga (2010) based on macroseismic observations from previous earthquakes (1636-2009). It can be noted that a region that released accumulated strain energy recently (<50 years) requires time to build strain to cause similar or larger earthquakes (Anbazhagan et al., 2012). So, considering the location of the higher seismic zone for the recent earthquake occurred, the region may need to be revisited according to Elastic Rebound Theory. In any case, the region with high-intensity values corresponds to the severity of the potential damages in the Himalayan region.

https://doi.org/10.63898/EWMG7978
*Corresponding Author

Situated between the Indian and Eurasian tectonic plates, the Himalaya forms a convergent boundary and the globe's most extensive active thrust fault system. Reverse slip faults prevail throughout the Himalayan region, accompanied by strike-slip faults in Indo-Burmese. The Indian and Eurasian plates converge at 40-50 mm/yr, primarily causing the central Himalayan region's seismicity. Seismicity in the eastern Himalayas is mainly due to the Indian plate's relative movement (≈ 35 mm/yr) towards the Sunda plate. Future earthquake hazards, with significant tectonically active faults and seismic potential, can devastate a developing country like India as infrastructure and population grow. Several Himalayan earthquakes in recent decades have provided evidence of this. A few recently created Ground Motion Prediction Equations (GMPEs) for the Himalayan region are available for various earthquake magnitudes and distances but not for distinct soil sites (Anbazhagan et al. 2019). Furthermore, despite India's high seismic exposure and risk according to the global model, there is no model for predicting seismic damage or risk in the country. In a situation like this, the region's macroseismic intensity data is extremely useful for evaluating the effects of earthquakes. This study presents macroseismic Intensity equations for the Himalayas and sub-regions.

1. Maximum Intensity (I_{max}) vs. Magnitude (M_w)

Epicentral Intensity, I_0, usually correlates very well with an earthquake's Magnitude, Mw, if the focal depth is constant. But, due to the problem associated with the determination of epicentral Intensity, I_0 (Musson 2005), we have adopted the criteria of I_{max} (usually equal to I_0), as it is easier to identify. I_{max} vs. M_w relationship for a region can provide insights into constraining historical earthquakes' magnitude values and estimating the most damaging intensity values for future earthquakes, which can help in hazard analysis studies. In this study, similar values of maximum Intensity were observed at multiple locations for many earthquakes; hence, we chose the locations nearest to the epicentre but with maximum observed Intensity to get the relation between the maximum observed Intensity and the earthquake magnitude. I_{max} (generally I_0) for an earthquake and its corresponding Magnitude shows a positive relationship. This may not be the case for deep earthquakes or sites where soil conditions affects the Intensity present at a location for an earthquake of a smaller magnitude. Higher intensity values at locations other than the epicentre might sometimes be reported due to local site and liquefaction-induced effects.

2. Intensity Prediction Equations (IPEs)

Unlike instrumental ground motions recorded after an earthquake associated with hazards at a specific location, macroseismic Intensity indicates the damage after an earthquake in any area. In past studies, macroseismic data have been utilized for developing IPE (e.g., Atkinson and Wald 2007; Martin and Szeliga 2010) and the Ground-motion to Intensity Conversion Equations (GMICEs) (e.g., Du et al. 2019, Cramer 2020). The IPE gives the attenuation of Intensity (I) for a given earthquake, w.r.t. a distance measure like the hypocentral distance (Rhyp) or the epicentral distance (Repi). IPEs created for a region have been used to constrain historical pre-instrumental earthquakes' Magnitude and epicentral location (Szeliga et al., 2010). Studies conducted in the past to develop IPEs for the Himalayan region can be categorized into two types:

I. Based on a few events that occurred in a particular location, e.g., Chandra 1980; Ghosh and Mahajan 2011; Prajapati et al. 2013; Bharali et al. 2021.
II. Based on multiple events in the Himalayas, e.g., Ambraseys and Douglas 2004; Szeliga et al. 2010.

These relationships are ad hoc and subject to constant modification, considering fresh information. For improved prediction outcomes, IPEs must be updated following notable earthquake events in each region. Selecting suitable functional forms, which may depend on data accessibility or the region-specific applicability of functional forms, is necessary to create IPEs. Anbazhagan and Thakur (2024) highlight relevant IPE forms from previous research for the Himalayas and other global regions. Based on the presumptions that the Intensity is proportional to the logarithm of the energy density or its power and that the seismic source is a point source, intensity attenuation with distance for IPEs is characterized in terms of epicentral Intensity (I_0) (Howell and Schultz 1975). Certain IPEs are expressed in terms of a distance metric (R) and an earthquake magnitude (M). Different functional forms of IPEs and models developed for Himalaya and its sub-regions are presented in Anbazhagan and Thakur (2024). In the present study, we have presented Magnitude (M_w) vs. maximum Intensity (I_{max}) equations which can be used to estimate the Magnitude for past earthquakes. Next, maximum Intensity (I_{max}) vs magnitude (M_w) relation has been given,

which can be used to get an estimate of epicentral Intensity for future events. IPEs from Anbazhagan and Thakur (2024) have also been presented, which can be used for earthquake risk estimation.

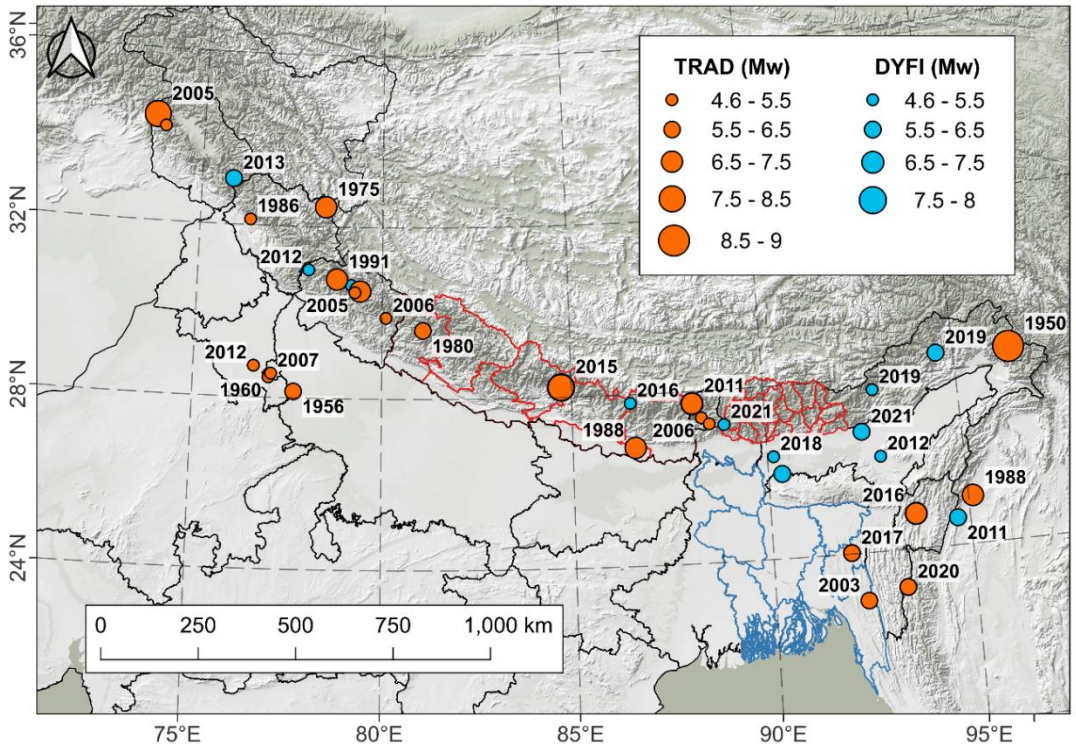

Fig. 1 The Himalayan Region map showing events location for TRAD and DYFI datasets

DATASET

The quality of macroseismic data of an event may be determined by several factors, as well as the degree of precision in reporting the position of the assigned value and the observer's level of expertise. Depending on the methodology, Allen et al. (2008) established the following quality score (best to lowest) for the macroseismic data:

I. Intensity Data Points (IDPs), i.e. intensities with location information.

II. Digitized historical or modern intensity maps.

III. Using a questionnaire format such as Did You Feel It? (or DYFI?)

IV. Digitized isoseismal maps.

I, II, and IV refer to traditional sources, whereas III is an internet-based questionnaire. In the present study, we have used two datasets - one containing Intensities from traditional sources based on IDPs (named TRAD) and another based on DYFI reports. This dataset naming (i.e., TRAD and DYFI) is the same as Hough and Martin's (2021). Figure 1 shows the epicentral location of the events considered for both datasets occurring between 1950-2021. Macroseismic data published in past studies has been utilized to prepare the final TRAD catalogue. Tables 2 and 3 in Anbazhagan and Thakur (2024) list all the events considered for IPE development. Since earthquake macroseismic data points are available in many intensity scales, using the data requires an equivalency between the scales. Musson et al. (2010) have given a conversion relation between different scales and European Macroseismic Scale -98 or EMS-98 (Grünthal et al. 1998) to use historical and current data available in different datasets under a single scale for analysis.

In the current study, we utilized historical and current data from other datasets under a single scale for analysis by using the conversion relation provided by Musson et al. (2010) between other scales and EMS-98. Criteria for reassessment and inclusion of the reported Intensities in our final TRAD dataset are described in Anbazhagan and Thakur (2024). In the final macroseismic catalogue, we have 5742 and 1317 data points for TRAD and DYFI, respectively. The maximum Intensity reported in both datasets is IX on the EMS-98 scale. For TRAD and DYFI datasets, 72.5% and 91.8% of IDPs are below Intensity VI (EMS-98), respectively (Figure 2 (a), (b)), which indicates that the TRAD intensities may be more suitable for predicting Intensities at higher levels as more accounts are available for these values.

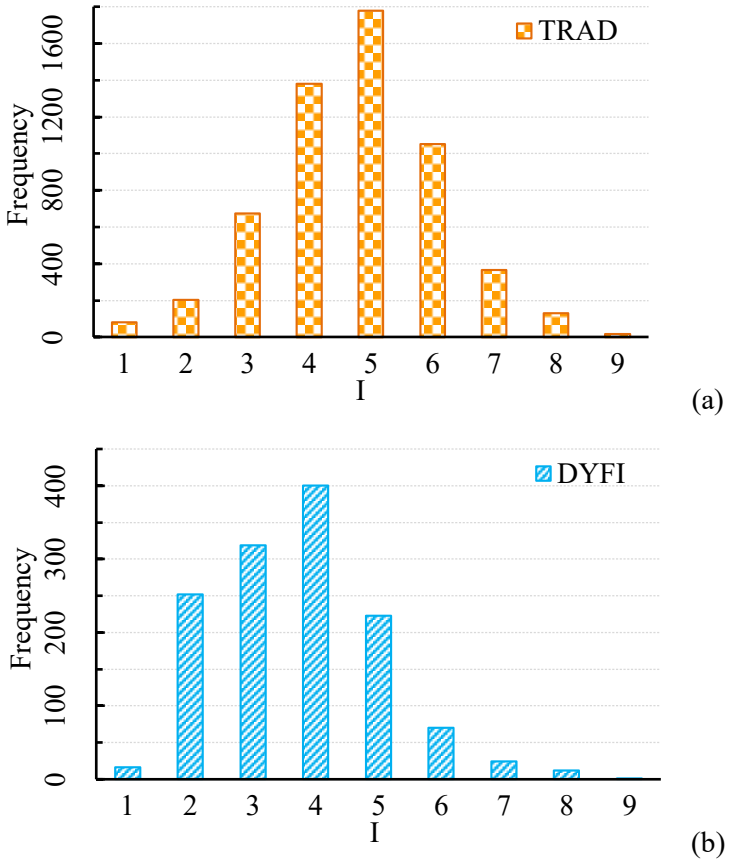

Fig. 2 Macroseismic Intensity vs frequency plot for the final catalogued (a) TRAD and (b) DYFI datasets, respectively

METHODOLOGY

1. Maximum Intensity and Magnitude Relationships

Past studies have used macroseismic data to constrain the Magnitude and location of historical earthquakes (Ambraseys and Douglas 2004; Szeliga et al. 2010). Usually, for this purpose, whole or partial (containing I_{max} observations only) macroseismic dataset is utilized as IDPs to obtain the approximate value of Magnitude and epicentral location (Kouskouna et al. 2020). Some studies have also used isoseismal areas between different intensity contours to approximate the earthquake's Magnitude (Musson 1996). Most of these studies focus mostly on Magnitude and epicentral location estimation. One important parameter that is difficult to constrain solely based on the macroseismic data is focal depth, which influences the magnitude estimation directly. As per Howell and Schultz's (1975) interpretation of Intensity values (assuming Intensity to be a measure of seismic energy density), if the focal depth is unknown, then the uncertainty in constrained values of Magnitude should be very high if the number of IDPs reported is similar in number for any two events. In the present study, we use I_{max} as a proxy for the earthquake's Magnitude, based on Howell and Schultz's (1975) hypothesis that epicentral Intensity (or I_{max} for historical earthquakes) is an indicator of energy release at the source (a point source approximation). For this purpose, both datasets (TRAD and DYFI) have been utilized. A first and second-order fit between Mw and Imax has been developed using a linear regression procedure.

2. Intensity Prediction Equations

A Two-Stage Regression Analysis (TSRA) method, as described by Joyner and Boore (1981) and a multiple regression analysis (MRA) procedure have been used to develop new IPES for the Himalayas and its different regions. The following functional form has been used:

$$I = a + bM + cM^2 + dR + e\ ln(R) \quad (1)$$

Where M = Event's Magnitude

R = Hypocentral distance

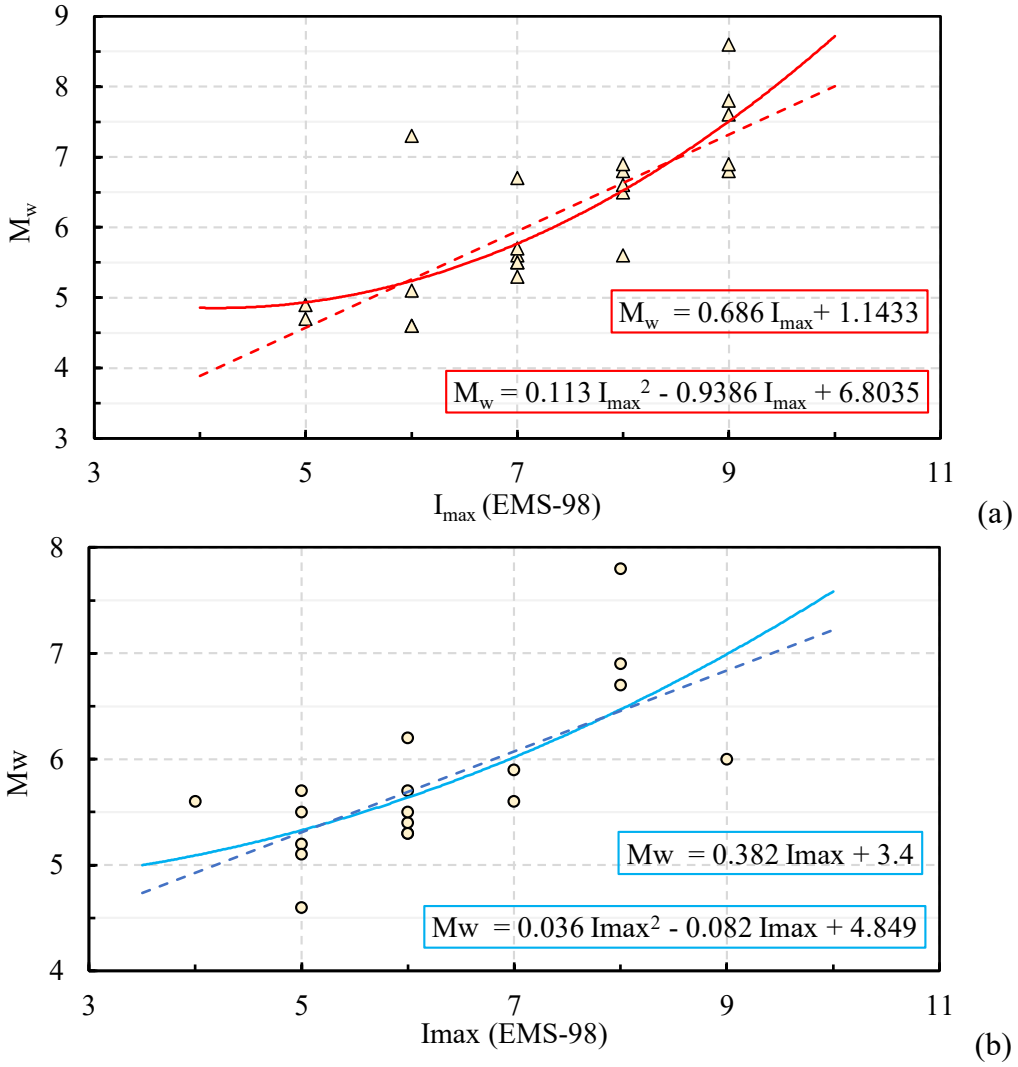

Fig. 3 Variation of Magnitude (Mw) with maximum Intensity (I_{max}) for the earthquake events in TRAD and DYFI datasets. First (linear)- and second-order (quadratic) relation between I_{max} and M_w has been given in blue for DYFI and in red for the TRAD dataset

Here, we used moment magnitude (M_w) and the new generalized moment magnitude scale (M_{wg}), also known as the Das magnitude scale developed by Das et al. (2019). The relationship between M_w and M_{wg} (Anbazhagan and Thakur 2024) used for the present study is given as:

$$M_{wg} = 1.103M_w - 0.878 \quad (2)$$

IPE's range of applicability in terms of both the M_w and M_{wg} scale has been calculated using the above relation.

RESULTS AND DISCUSSION

1. Maximum Intensity (I_{max}) vs. Magnitude (M_w)

A first and second-order fit between M_w and I_{max} has been developed using simple linear regression (Figure 3). We have chosen a second-order fit here to highlight that if one assumes a constant focal depth of occurrence of the events, then the M_w estimate should rise asymptotically for higher I_{max} values based on the assumption that Intensity assignment will saturate for higher magnitudes instead of linearly increasing. These second-order relations are:

$$M_w(TRAD) = 6.804 - 0.939I_{max} + 0.113I_{max}^2 \quad (3)$$
$$4.6 \leq M_w \leq 8.6; R^2 = 0.64; \sigma = 0.71$$

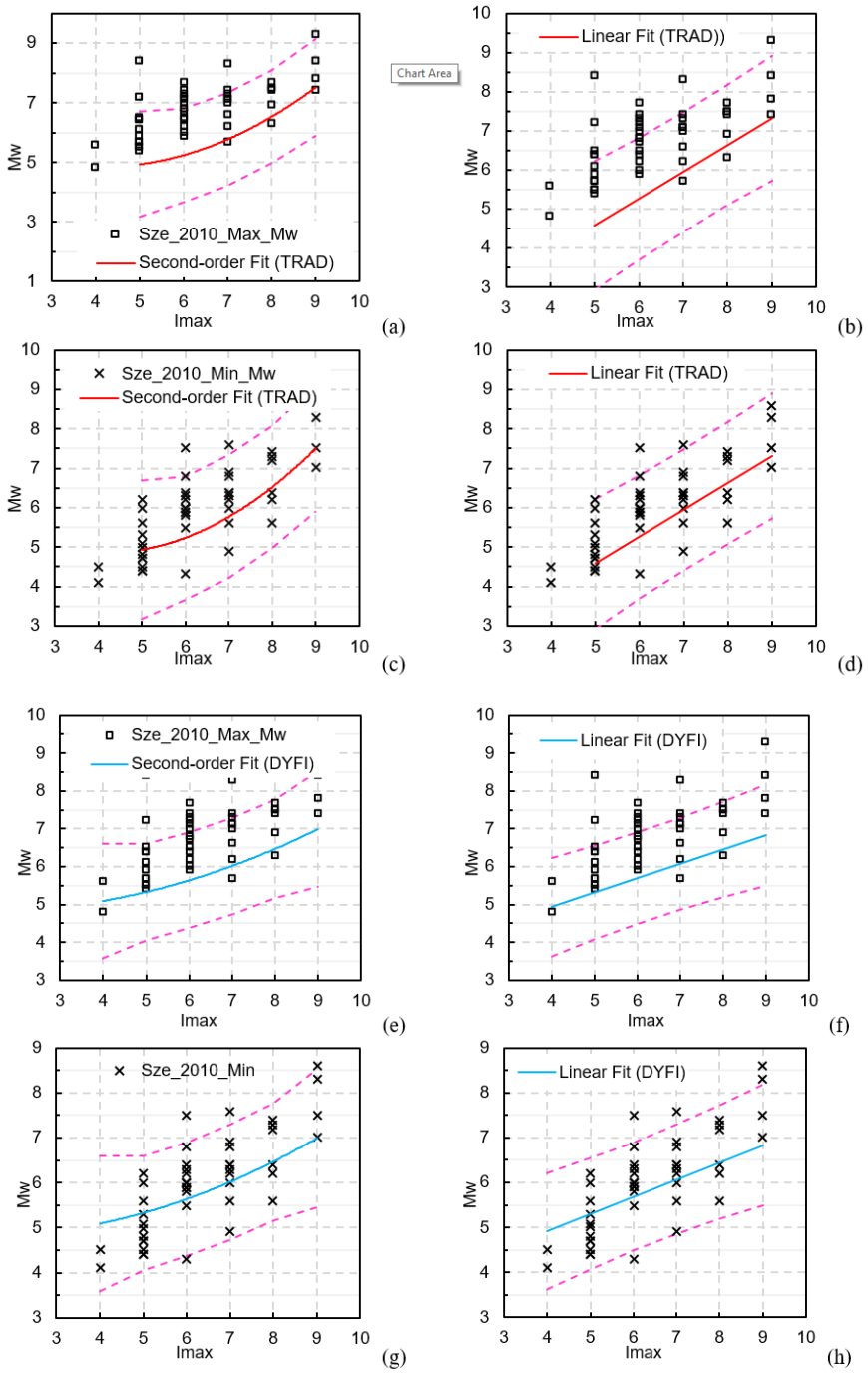

Fig. 4 Plots of I_{max} vs. M_w first (linear) and second-order fit obtained from the TRAD dataset considering events between 1950 and 2020. Maximum (Sze_2010_Max_Mw) and minimum Magnitude (Sze_2010_Min_Mw) estimates for 48 historic Himalayan events (occurred between 1762 and 1947) given by Szeliga et al. (2010) using Bakun and Wentworth (1997) method have also been shown. 95% prediction interval are shown with dotted lines

$$M_w(DYFI) = 4.849 - 0.082I_{max} + 0.036I_{max}^2 \quad (4)$$
$$4.6 \leq M_w \leq 7.8; R^2 = 0.49; \sigma = 0.57$$

To compare these estimates with previous estimates by Szeliga et al. (2010) for the Himalayan region, these relationships with their mean and 95% prediction interval estimates are shown in Figure 4. We have used the prediction interval formula since there is more uncertainty in predicting M_w from a given value of I_{max} as compared to the mean M_w value calculated by equations (3) and (4). Instead of the mean response of the response variable (here, M_w), these prediction intervals correspond to the prediction of the response variable at any chosen value of the predictor variable (i.e., I_{max}). These 95% prediction intervals

are based on the formula for the standard error of predicted value $\hat{y}_o$, *s.e.* $(\hat{y}_o)$ at a given value of predictor x_0 with mean $\bar{x}$, from Chatterjee and Hadi (2013) given as:

$$s.e.(\widehat{y_0}) = \hat{\sigma}\left(\sqrt{1 + \left(\frac{1}{n}\right) + \left(\frac{(x_0 - \bar{x})^2}{\sum(x_i - \bar{x})^2}\right)}\right) \quad (5)$$

Here $\hat{\sigma}$ is the mean squared error of y, and n is the total number of observations. Confidence limits for the $(1-\alpha)\times 100\%$ confidence coefficient for the predicted value is calculated as

$$s\widehat{y_0} \pm t_{n-2,\frac{\alpha}{2}}\, s.e.(\widehat{y_0})$$

where $t_{n-2,\alpha/2}$ represents $(1-\alpha/2)$ percentile of a t distribution with $(n-2)$ degrees of freedom. To estimate the M_w for a given event, Szeliga et al. (2010) used Bakun and Wentworth's (1997) method while utilizing the event's whole macroseismic data to find these estimates. They have given maximum and minimum values of magnitude estimates while giving more weightage to the epicentre's location and magnitude estimation. From Figure 4, it can be observed that using I_{max} as a measure for estimating M_w give consistently lesser values for maximum magnitude estimates of Szeliga et al. (2010), while yielding comparable estimates for minimum magnitude values. Although considering the usual lack of information on focal depth of historic events these relations can be used as a first-order estimate for the events' Magnitude.

2. Future Maximum Intensity Predictions

Next, we considered a relation between I_{max} and M_w to predict I_{max} for future earthquake scenarios. Both first-order and second-order relationships have been developed. From a statistical point of view (considering R^2 values only), there is not much advantage of using one over the other. However, a rationale has been developed in the following paragraphs while considering building data types for the region to choose between the two. Saturation behaviour in the I_{max} values at higher M_w values is observed when a second-order fit is considered (Figure 5). One possible explanation of the saturation of I_{max} can be based on the region's building stock and its damage. We have used BMTPC (2019) data for the analysis, which has collected its Housing data from the 2011 Census conducted by the Government of India (GOI). We have collected district-wise data for the I_{max} locations situated in India from BMTPC (2019), which provides information about the number of houses in the district where I_{max} is reported and the types of houses categorized along the lines of MSK-64 'Type of structures (Buildings)' classification scheme. Suppose one reasonably assumes that building stock percentages when these earthquakes occurred would be similar or higher for lower categories (such as W_A, W_B, and W_X). In that case, one can make the following inferences.

From the data in Table 1, for TRAD events' I_{max} locations (district-wise data), only 4.8% ('Total') of buildings have reinforced walls or well-built wooden structures (W_C in Table 1). Around 57.6% (average) of houses have walls built with "Burnt Brick Wall & Stone wall packed with mortar" (W_B) description. Other houses' categories (W_X) usually have weaker materials or poor workmanship (around 18.3%). For the DYFI dataset (Table 2), 46.6% of houses are under W_X (light structures), 38.4% in W_B, and 9.5% in W_A. These buildings (W_A, W_B, and W_C) come under Vulnerability classes A, B, and C on the EMS-98 scale (Table 2). Also, the damage description of many I_{max} values shows that most damaged buildings are in Vulnerability classes A, B, and C as per EMS-98. So, at higher magnitudes, the I_{max} values will saturate because of the presence of the higher percentage of building stock (W_A, W_B, and W_X), for which even if the damage description increases from a "few" to "many" (see EMS-98) the Intensity value won't reach the higher Intensity description of the EMS-98.

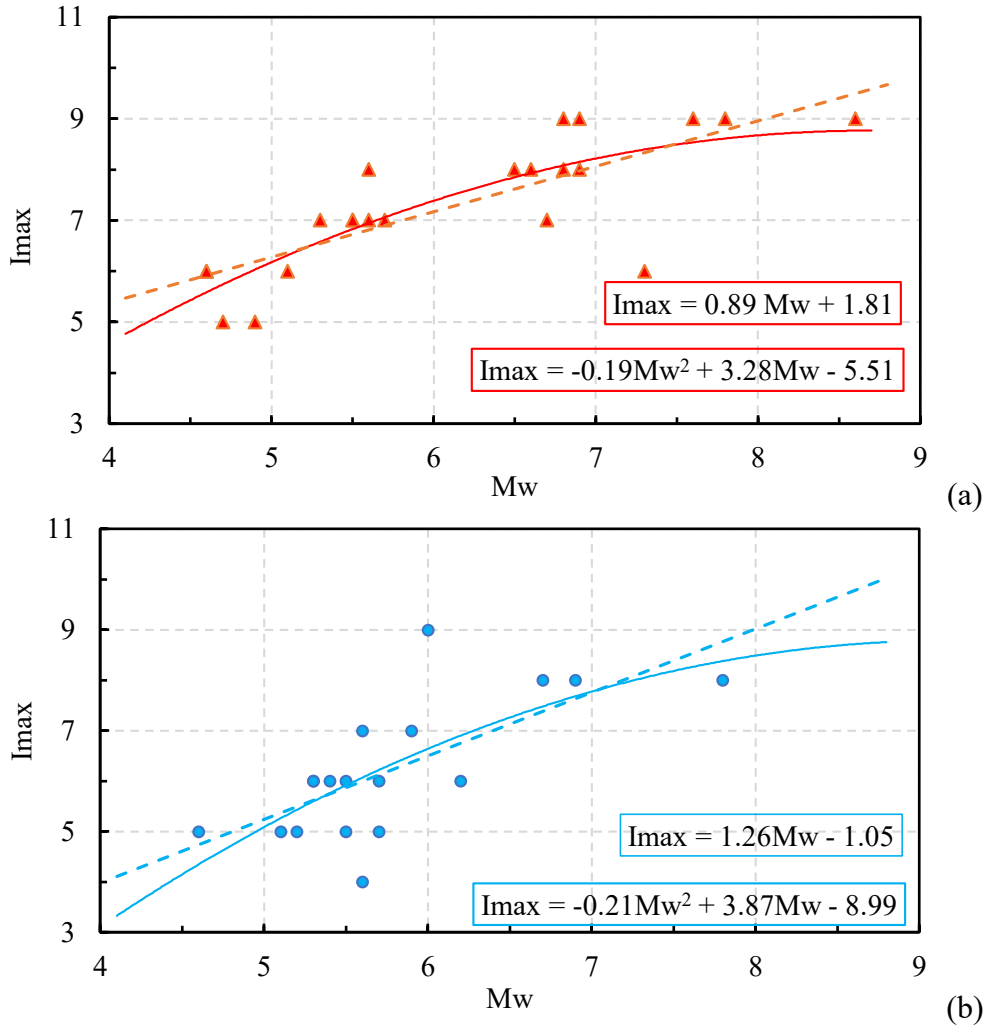

Fig. 5 Variation of maximum Intensity (I_{max}) with Magnitude (M_w) for the earthquake events in (a) TRAD and (b) DYFI datasets. First (linear)- and second-order (quadratic) relationships between I_{max} and M_w have been given in (a) for the TRAD and in (b) for the DYFI dataset

Table 1: Data of different house types based on their wall types (WA, WB, WC, and WX) and roof types (R1, R2, and R3), in percentage from BMTPC (2019) for the districts where Imax was reported in the TRAD dataset. WA, WB, WC, and WX correspond to wall 'Category -A,' 'Category-B,' and 'Category – C,' and R1, R2, and R3 correspond to the similarly named roof categories in BMTPC (2019). BD – Bangladesh; N – Nepal; UT – Union Territory of India

Earthquake	State/ Province	District	I_{max}	W_A	W_B	W_C	W_X	R1	R2	R3
ASSAM-1950	Arunachal Pradesh	Anjaw	9	1.7	1	20	77.3	98.8	0.7	0.4
KINNAUR-1975	Himachal Pradesh	Kinnaur	8	24.1	58.7	12.9	4.2	73.1	12.1	14.8
BAJHANG-1980	Sudurpashchim (N)	Bajhang	8	-	-	-	-	-	-	-
DHARAMSALA-1986	Himachal Pradesh	Kangra	7	45.2	52.8	0.7	1.3	6.8	51.9	41.3
INDO-BURMA-1988	Manipur	Ukhrul	6	13.8	3.9	74.3	8	97.7	1.1	1.2
UDAYPUR-1988	Bihar	Madubani	8	11	44.4	0.9	43.6	63.3	14.8	22
UTTARKASHI-1991	Uttarakhand	Uttarkashi	9	33.4	54.4	10	2.2	20.4	40.8	38.9
CHAMOLI-1999	Uttarakhand	Chamoli	8	42.5	54.5	1.5	1.4	12.1	51.1	36.8
KOLABONIA-2003	Chittagong (BD)	Rangamati	7	-	-	-	-	-	-	-
KASHMIR-2005	Muzaffarabad	Muzaffarabad	9	-	-	-	-	-	-	-
GHARWAL-2005-B	Uttarakhand	Rudraprayag	6	46	51.8	1.4	0.8	8.9	45.7	45.4

SIKKIM-2006	Sikkim	East District	7	10.8	39.4	35.6	14.2	61.3	1.6	37.3
KUMAON-2006-B	Uttarakhand	Pithoragarh	6	14.2	82.8	2.2	0.8	9.9	40.8	49.3
SIKKIM-2007-B	Sikkim	South District	5	16.2	25.4	40.4	17.9	78.2	1.2	20.7
DELHI-2007	Delhi (UT)	South	5	3.8	89.8	5.4	1	10.4	17.1	72.5
KASHMIR-2009-A	Muzaffarabad	Muzaffarabad	7	-	-	-	-	-	-	-
SIKKIM-2011	Sikkim	West District	9	22.3	18.1	37.3	22.3	88.2	1.2	10.6
DELHI-2012	Haryana	Jhajjar	6	4.7	92.5	2	0.8	15	55.5	29.5
NEPAL-2015	Bagmati (N)	Rasuwa	9	-	-	-	-	-	-	-
MANIPUR-2016	Manipur	Tamenglong	7	31.5	3.8	16.4	48.3	96.7	2.3	1
TRIPURA-2017	Tripura	North Tripura	7	29.6	20.2	1	49.2	94.2	1.1	4.7
MIZORAM-2020	Mizoram	Champai	8	0.6	4.5	11.6	83.3	93.4	1.4	5.2
Total (in percentage)				19.3	57.6	4.8	18.3	36.3	27.0	36.7

Table 2: Data of different house types based on their wall types (WA, WB, WC, and WX) and roof types (R1, R2, and R3) in percentage from BMTPC (2019) for the districts where Imax was reported in the DYFI dataset. WA, WB, WC, and WX correspond to wall 'Category -A,' 'Category-B,' and 'Category – C,' and R1, R2, and R3 correspond to the similarly named roof categories in BMTPC (2019). N – Nepal

Earthquake	State/ Province	District	I_{max}	W_A	W_B	W_C	W_X	R1	R2	R3
INDO-MYANMAR-2011	Manipur	Thoubal	6	69.4	7.9	1	21.7	96.2	1.7	2
SIKKIM-2011	Sikkim	North District	8	8.2	14.4	51.8	25.6	80.5	3	16.5
UTTARAKHAND-2012	Uttarakhand	Uttarkashi	6	33.4	54.4	10	2.2	20.4	40.8	38.9
DELHI-2012	Haryana	Rohtak	5	3.5	94.6	1.4	0.5	26.9	31.1	42.1
ASSAM-2012	Assam	Nagaon	6	4.5	21.4	6.2	67.9	96.8	1	2.2
JAMMU-2013	Punjab	Jalandhar	5	4.1	89.2	6	0.8	7.9	11.4	80.7
NEPAL-2015	Bagmati (N)	Nuwakot	8	-	-	-	-	-	-	-
MANIPUR-2016	Assam	Hailakandi	8	7.1	26.9	4.9	61.2	95.4	2.3	2.4
NEPAL-2016	Bagmati (N)	Dolakha	5	-	-	-	-	-	-	-
TRIPURA-2017	Tripura	Dhalai	6	42.6	9.8	0.5	47.1	96.3	1.2	2.5
UTTARAKHAND-2017	Uttarakhand	Chamoli	5	42.5	54.5	1.5	1.4	12.1	51.1	36.8
ASSAM-2018	Assam	Kokrajhar	6	7.9	15.1	8.4	68.6	92.8	5.7	1.5
ARUNACHAL-2019A	Assam	Jorhat	7	2.8	28.9	2.2	66	93.5	2.1	4.4
ARUNACHAL-2019B	Arunachal Pradesh	Lower Subansiri	5	2.3	5.4	27.4	65	92.5	1.5	5.9
MIZORAM-2020	Mizoram	Champhai	4	0.6	4.5	11.6	83.3	93.4	1.4	5.2
SIKKIM-2021	Sikkim	East District	6	10.8	39.4	35.6	14.2	61.3	1.6	37.3
ASSAM-2021	Assam	Udalgiri	9	2.8	17.8	3.6	75.8	98.4	1.1	0.5
MEGHALAYA-2021	Assam	Dhubri	7	2.5	11.3	4.3	81.9	92.8	5.7	1.5
Total (in percentage)				9.5	38.4	5.5	46.6	69.7	9.3	21.0

Another aspect that can be a possible explanation for this saturation is a bias in Intensity reporting. Usually, more reports will come from locations where infrastructure is poor as such buildings are more damage-prone to earthquakes, leading to under-reporting of the damage to buildings with earthquake-resistant design elements (Hough 2013). Hence, even if the earthquake magnitude increases and corresponding reported damage to poor infrastructure also relatively increases, which, when assigned as per EMS-98, will lead to saturation in I_{max} values. So, it becomes the responsibility of the field observer to report damage observed in all kinds of buildings. While assigning the Intensity as per EMS-98, "Definitions of quantity" should be used appropriately. For internet-based questionnaires like DYFI, this bias will persist more if due care is not taken in quantifying damage to different types of buildings (w.r.t their total numbers)

while assigning Intensity. Due to these reasons, we propose a second-order Magnitude fit to capture the saturation effect (of I_{max}) rather than a linear one (Figure 6). The second-order relation between maximum observed Intensity (I_{max}) and Magnitude (M_w) is given:

$$I_{max}(TRAD) = -5.51 + 3.28M_w - 0.19M_w^2 \quad (6)$$
$$4.6 \leq M_w \leq 8.6; R^2 = 0.61; \sigma = 0.8$$

$$I_{max}(DYFI) = -8.99 + 3.87M_w - 0.21M_w^2 \quad (7)$$
$$4.6 \leq M_w \leq 7.8; R^2 = 0.49; \sigma = 1.0$$

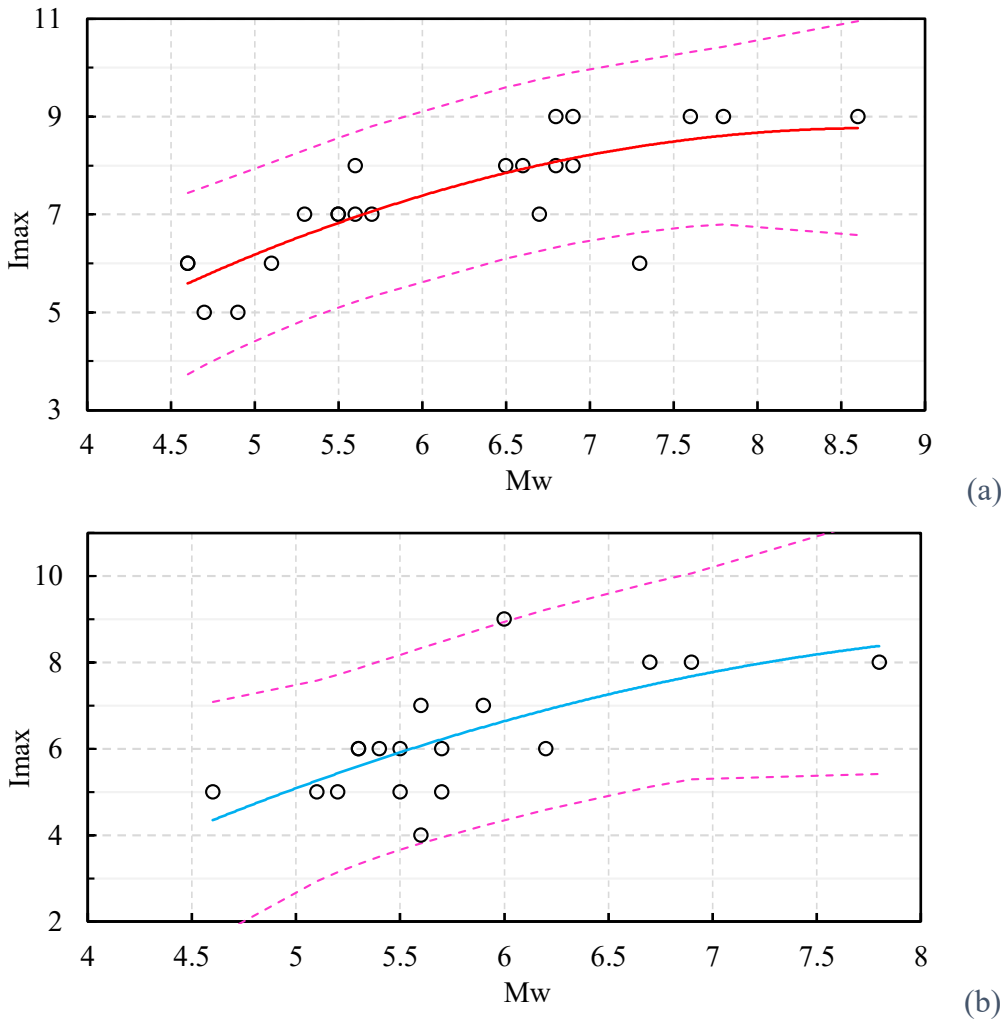

Fig. 6 I_{max} vs M_w relationship developed using (a) TRAD and (b) DYFI dataset proposed for future prediction of Imax along with 95% prediction intervals (dotted lines)

Even though I_{max} vs M_w relations are required for intensity prediction, their application in risk estimation is limited. IPEs are essential to risk estimation and mapping in the region; as highlighted earlier, there are very limited IPEs for the Himalayan region. Hence, we developed new IPEs for the Himalayan and sub-regions after systematically synchronizing intensity data and models. More details about the study are explained in Anbazhagan and Thakur (2024). A summary of the IPEs developed is presented here.

Himalayan Region IPEs

For the Himalayan region, the IPEs developed by Anbazhagan and Thakur (2024) are:

$$I(TRAD) = -4.01 + 3.46M - 0.21M^2 - 0.0012R_{hyp} - 0.87\ln(R_{hyp}) \quad (8)$$
$$here\ M \in \begin{cases} 4.6 \leq M_w \leq 8.6 & if\ M = M_w \\ 4.2 \leq M_{wg} \leq 8.6 & if\ M = M_{wg}' \end{cases}$$
$$R^2 = 0.56, \sigma = 0.91$$

$$I(DYFI) = 0.14 + 2.22M - 0.11M^2 - 0.00003R_{hyp} - 1.04\ln(R_{hyp}) \quad (9)$$

$$here\ M \in \begin{cases} 4.6 \le M_w \le 7.8 & if\ M = M_w \\ 4.2 \le M_{wg} \le 7.7 & if\ M = M_{wg}' \end{cases}$$
$$R^2 = 0.31, \sigma = 1.10$$

N-W Himalaya

IPEs using TSRA are:

$$I(TRAD) = 5.93 + 0.085M_w + 0.09M_w^2 - 0.0013R_{hyp} - 1.05\ln(R_{hyp}) \quad (10)$$
$$4.6 \le M_w \le 7.6, R^2 = 0.75, \sigma = 0.78$$
$$I(DYFI) = 233.76 - 85.24M_w + 7.95M_w^2 - 0.0006R_{hyp} - 0.45\ln(R_{hyp}) \quad (11)$$
$$5.1 \le M_w \le 5.7, R^2 = 0.15, \sigma = 0.89$$

Central Himalaya

Developed IPEs for the Central Himalayas are:

$$I(TRAD) = 0.70 + 1.63M_w - 0.046M_w^2 - 0.0013R_{hyp} - 0.84\ln(R_{hyp}) \quad (12)$$
$$4.6 \le M_w \le 7.8, R^2 = 0.47, \sigma = 0.96$$
$$I(DYFI) = 3.19 + 1.27M_w - 0.036M_w^2 - 0.00017R_{hyp} - 1.06\ln(R_{hyp}) \quad (13)$$
$$4.6 \le M_w \le 7.8, R^2 = 0.32, \sigma = 1.12$$

N-E Himalaya

IPEs using MRA and TSRA results for TRAD and DYFI, respectively, are:

$$I(TRAD) = 3.58 + 1.37M_w - 0.058M_w^2 - 0.0008R_{hyp} - 0.92\ln(R_{hyp}) \quad (14)$$
$$5.6 \le M_w \le 8.6, R^2 = 0.58, \sigma = 0.91$$
$$I(DYFI) = -6.96 + 5.00M_w - 0.34M_w^2 + 0.00079R_{hyp} - 1.33\ln(R_{hyp}) \quad (15)$$
$$5.4 \le M_w \le 6.7, R^2 = 0.31, \sigma = 1.07$$

3. Comparison of IPEs with Past Studies

Ambraseys and Douglas (2004) or A&D04, and Szeliga et al. (2010) or Sze10 have developed IPEs for the Himalayas utilizing data from traditional sources. Allen et al. (2012) have developed IPEs for active crustal areas (including the Himalayas) using global macroseismic data. The IPEs they use differ slightly from those given in Equation 1. For comparison with our IPEs, we have used the IPE given by Allen et al. (2012) for Rhyp (hereafter Allen12). In comparison to TRAD IPE (Equation 8), A&D04 shows higher anelastic attenuation over the far-site distances (>100 km) for various magnitudes (Figure 7), whereas for Sze10, Allen12 and DYFI, this effect is negligible. For near-site distances, Intensity attenuation due to geometric spreading is highest in Sze10, followed by (in order) Allen12, A&D04, and DYFI. A&D04 and Sze10 predict epicentral Intensities (I_0) 1-2 units higher (for Mw 8.0) than TRAD and DYFI. For Mw 5.0, I_0 is expected by A&D04 and DYFI matches, whereas those indicated by Sze10 are almost a unit higher. Allen et al. (2012) have mentioned that their IPEs underestimate the Intensity for Mw 5.0-5.5, the possible cause of which is the lack of low-intensity IDPs at far-site distances. The scaling of I_0 w.r.t. Mw has the highest Magnitude for A&D10 and the lowest for the DYFI dataset. The difference in predicted TRAD and DYFI intensities remains almost the same (<0.5 Intensity units) for the entire Mw (5-8) range.

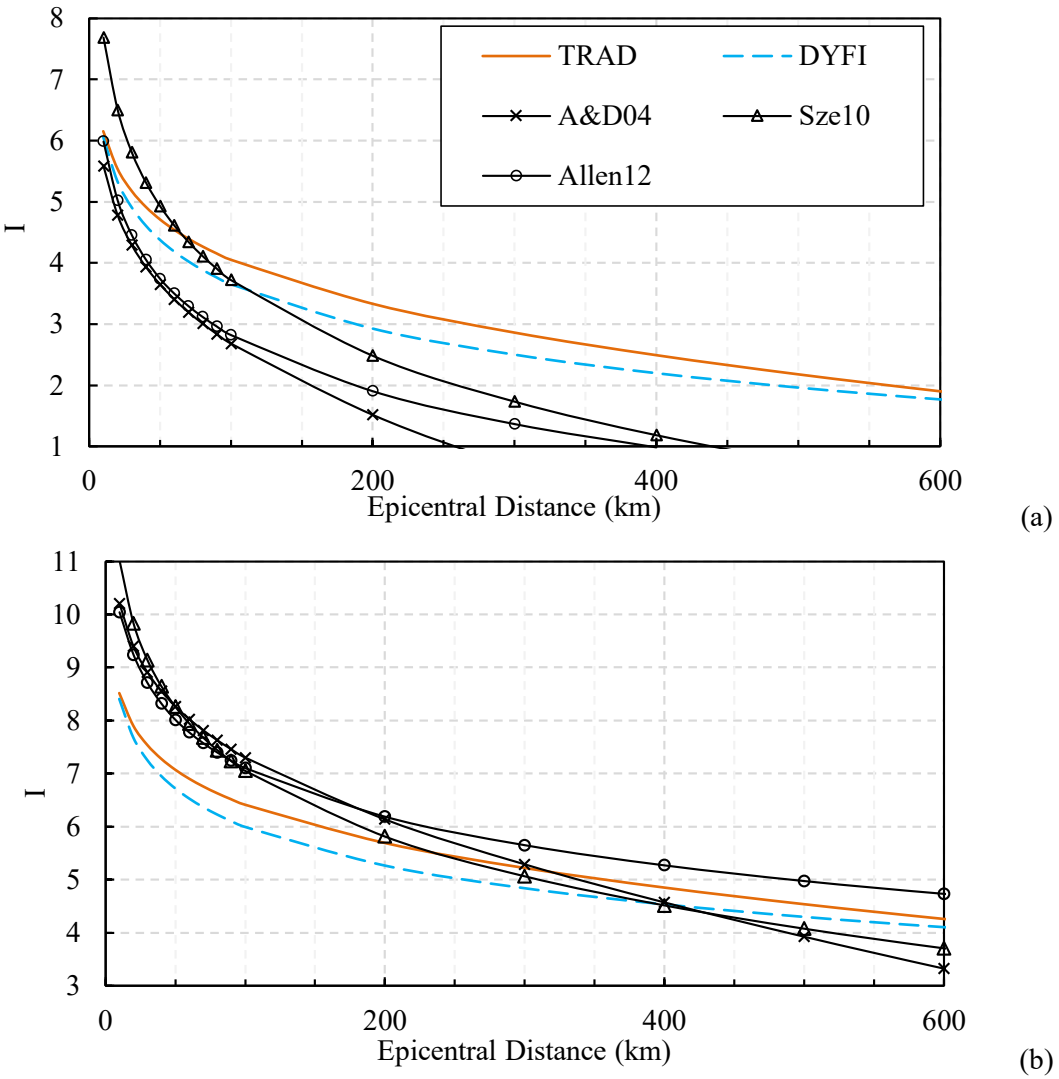

Fig. 7 Comparison between different IPEs for hypothetical earthquakes of Magnitude (a) Mw 5.0 and (b) Mw 8.0

If we compare the IPEs developed for sub-regions of the Himalayas (Figure 8), for lower Magnitude (Mw 5.0), Intensities predicted by N-E Himalayan TRAD IPE (Equation 14) are consistently higher as compared to the other two regions between Mw 5.0-8.0. Attenuation due to geometric spreading is slightly higher (Figure 8) for N-W Himalaya than the other two areas for TRAD-based IPEs. DYFI-based IPE for N-W Himalaya (Equation 11) and N-E Himalaya (Equation 15) show a considerable deviation in Figure 8 from those predicted by corresponding TRAD-based IPEs (Equations 10 and 14). This is due to the limited magnitude range of applicability for both IPEs compared to their TRAD-based counterparts. Hence, we recommend considering the Mw (or Mwg) range while using these IPEs. The Central Himalayan IPEs (Equations 12 and 13) predict similar Intensities for Mw 5.0 – 8.0. At Mw 8.0, N-W TRAD IPE predicted consistently higher Intensities than all other IPEs, possibly due to the type of building infrastructure in these regions.

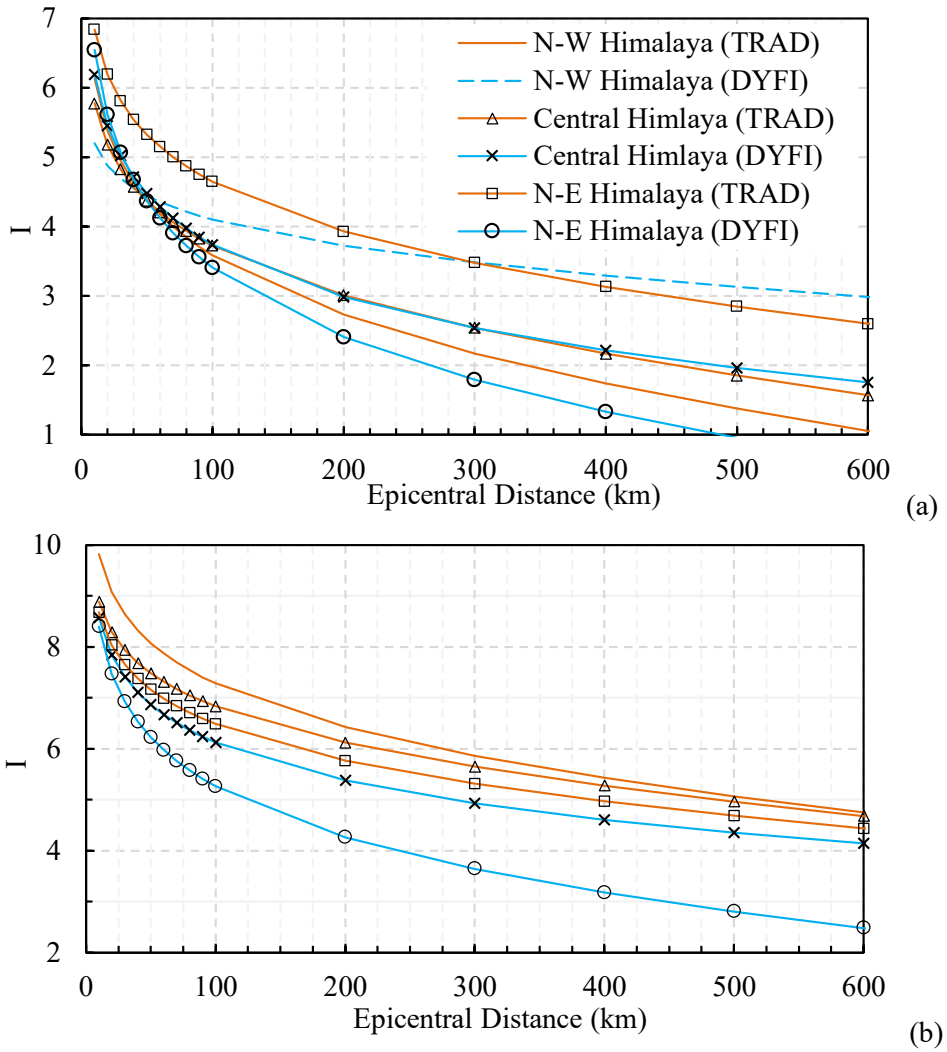

Fig. 8 Comparison between newly developed IPEs for the Himalayan region for events with magnitude (a) Mw 5.0 and (b) Mw 8.0. TRAD-based IPEs are in orange, whereas DYFI-based IPEs are in blue

CONCLUSIONS

To predict earthquake macroseismic intensity for the Himalayas, macroseismic data for the events (1950-2020) from traditional sources (or TRAD) and between 2011 and 2021 from the USGS DYFI online database have been utilized to create the magnitude and intensity predictive equations. Second-order relationships were developed between maximum Intensity and earthquake Magnitude for two scenarios: estimation of maximum Intensity for future earthquakes and constraining past earthquakes' Magnitude based on maximum Intensity. Developed relations are:

M_w vs I_{max} – for historic earthquakes' Mw estimation

$$M_w(TRAD) = 6.804 - 0.939I_{max} + 0.113I_{max}^2 \quad (16)$$
$$4.6 \leq M_w \leq 8.6; R^2 = 0.64; \sigma = 0.71$$

$$M_w(TRAD) = 4.849 - 0.082I_{max} + 0.036I_{max}^2 \quad (17)$$
$$4.6 \leq M_w \leq 7.8; R^2 = 0.49; \sigma = 0.57$$

I_{max} vs M_w – for future earthquakes' Imax estimation

$$I_{max}(TRAD) = -5.51 + 3.28M_w - 0.19M_w^2 \quad (18)$$
$$4.6 \leq M_w \leq 8.6; R^2 = 0.61; \sigma = 0.8$$

$$I_{max}(DYFI) = -8.99 + 3.87M_w - 0.21M_w^2 \quad (19)$$
$$4.6 \leq M_w \leq 7.8; R^2 = 0.49; \sigma = 1.0$$

Next, IPE developed using a two-stage regression method (based on Joyner and Boore, 1981) and a multiple linear regression analysis are presented. Nevertheless, their capability for the prediction did not

differ significantly. The development of IPEs used Magnitude first and second-order relationships; in addition to providing appropriate range equations for Mw and Mwg, IPEs used Mw and generalized moment magnitude scale (Mwg).

These relations for future predictions of maximum Intensity and estimating past earthquakes' magnitudes show a significant uncertainty, as reflected in their root-mean-squared error (RMSE) values. However, these relationships can be useful for obtaining first-order estimates and in situations where information is lacking. We have also highlighted how the regional infrastructure characteristics can lead to saturation behaviour in the maximum Intensity values observed for large earthquakes in the Himalayan region. The impact of future earthquakes in the area can be evaluated using these recently created IPEs. To separate the source and site effects in different regions, distinct IPEs were also developed for the Himalayan sub-regions. DYFI-based predicted intensities are consistently lower than their TRAD counterpart, according to a comparison of IPEs created from TRAD and DYFI data. This draws attention to a significant distinction between the two categories of macroseismic data that warrants additional study. Error terms in the IPEs presented here can be applied to probabilistic intensity mapping.

REFERENCES

1. Anbazhagan P., Prabhu, G. and Aditya P. (2012). "Seismic Hazard Map of Coimbatore using Subsurface Fault Rupture", *Natural Hazard*, Vol. 60, pp.1325-1345.
2. Anbazhagan P, Prabhu, G., Moustafa Sayed, S.R, Nassir, S. Arifi, Al and Aditya, P., (2014). "Provisions for Geotechnical Aspects and Soil Classification in Indian Seismic Design Code IS-1893", *Disaster Advances*, Vol. 7, No. 3, pp. 72-89.
3. Allen, T.I., Wald, D.J., Hotovec, A.J., Lin, K., Earle, P.S. and Marano, K.D. (2008). "An Atlas of ShakeMaps for Selected Global Earthquakes", *US Geological Survey Open-File Report,* Vol. 35, pp. 1236.
4. Allen, T.I., Wald, D.J. and Worden, C.B. (2012). "Intensity Attenuation for Active Crustal Regions", *J. Seismol*, Vol. 16, pp. 409–433. https://doi.org/10.1007/s10950-012-9278-7
5. Ambraseys, N.N., and Douglas, J. (2004). "Magnitude Calibration of north Indian Earthquakes", *Geophys. J. Int.,* Vol. 159, pp. 165–206. https://doi.org/10.1111/j.1365-246X.2004.02323.x
6. Anbazhagan, P., Bajaj K., Matharum K., Moustafa, S.S. and Al-Arifi, N.S. (2019). "Probabilistic Seismic Hazard Analysis using Logic Tree Approach - Patna District (India)", *Nat Hazards Earth Syst Sc*i, Vol. 19, pp. 2097–2115. https://doi.org/10.5194/nhess-19-2097-2019
7. Anbazhagan, P, and Thakur, H (2024). "Intensity Prediction Equations for Himalaya and its Sub-Regions Based on Data from Traditional Sources and USGS's Did You Feel It? (DYFI)", *Journal of Seismology*, Vol. 28, pp. 707-734.DoI: https://doi.org/10.1007/s10950-024-10214-7
8. Atkinson, G.M. and Wald, D.J. (2007). "Did You Feel It?" Intensity data: A Surprisingly Good Measure of Earthquake Ground Motion", *Seism. Res. Lett.*, Vol. 78, pp. 362-368. https://doi.org/10.1785/gssrl.78.3.362
9. Bakun, W.U. and Wentworth, C.M. (1997). "Estimating Earthquake Location and Magnitude from Seismic Intensity Data", *Bulletin of the Seismological Society of America*, Vol. 87, No. 6, pp. 1502-1521. https://doi.org/10.1785/BSSA0870061502
10. Bharali, B., Rakshit, R., Dinpuia, L., Saikia, S. and Baruah, S. (2021). "The 2020 Mw 5.5 Mizoram Earthquake and Associated Swarm Activity in the Junction of the Surma Basin and Indo-Myanmar Subduction Region", *Nat Hazards*, Vol. 109, pp. 2381–2398. https://doi.org/10.1007/s11069-021-04924-1
11. BMTPC, (2019). "Vulnerability Atlas of India – Earthquake, Wind, Flood, Landslide, Thunderstorm Maps and Damage Risk to Housing, Building Materials and Technology Promotion Council", *Ministry of Housing and Urban Affairs, Government of India*. Link: https://vai.bmtpc.org/
12. Chandra, U. (1980). "Attenuation of intensities in India", *In: Proceedings of the 7th World Conference on Earthquake Engineering*, Istanbul, Turkey, Vol 2. pp. 521–524.
13. Chatterjee, S. and Hadi, A.S. (2013). "Regression Analysis by Example", *John Wiley & Sons*.
14. Cramer, C.H. (2020). "Updated GMICE for Central and Eastern North America Extending to Higher Intensities", *Seism. Res. Lett.,* Vol. 91, No. 6, pp. 3518–3527. https://doi.org/10.1785/0220200061

15. Das, R., Sharma, M.L., Wason, H.R., Choudhury, D. and Gonzalez, G. (2019). "A Seismic Moment Magnitude Scale", *Bulletin of the Seismological Society of America*, Vol. 109, No. 4, pp. 1542-1555. https://doi.org/10.1785/0120180338
16. Du, K., Ding, B., Luo, H. and Sun, J. (2018). "Relationship between Peak Ground Acceleration, Peak Ground Velocity, and Macroseismic Intensity in Western China", *Bull. Seism. Soc. Am.*, Vol. 109, No. 1, pp. 284–297. https://doi.org/10.1785/0120180216
17. Ghosh, G.K. and Mahajan, A.K. (2011). "Interpretation of Intensity Attenuation Relation of 1905 Kangra Earthquake with Epicentral Distance and Magnitude in the Northwest Himalayan Region", *J Geol Soc India*, Vol. 77, No. 511–520. https://doi.org/10.1007/s12594-011-0058-8
18. Grünthal, G. and Leveret A. (Editors) (1998). "European macroseismic scale 1998 (EMS-98)", *Cahiers du Centre Européen de Géodynamique et de Séismologie, Luxembourg*, Vol. 15. doi: https://doi.org/10.2312/EMS-98.full.en
19. Hough, S.E. (2013). "Spatial variability of "Did You Feel It?" Intensity Data: Insights into Sampling Biases in Historical Earthquake Intensity Distributions", *Bull. Seismol. Soc. Am.,* Vol. 103, No. 5, pp. 2767–2781. https://doi.org/10.1785/0120120285
20. Hough, S.E. and Martin, S.S. (2021). "Which Earthquake Accounts Matter? Seism", *Res. Lett.*, Vol. 92, No. 2A, pp. 1069–1084. https://doi.org/10.1785/0220200366
21. Howell, B.F. and Schultz, T.R. (1975). "Attenuation of Modified Mercalli Intensity with Distance from the Epicenter", *Bull. Seism. Soc. Am.*, Vol. 65, No. 3, pp. 651-665. https://doi.org/10.1785/BSSA0650030651
22. Joyner, W.B. and Boore, D.M. (1981). "Peak Horizontal Acceleration and Velocity from Strong-Motion Records Including Records from the 1979 Imperial Valley", *California, earthquake; Bulletin of the Seismological Society of America*, Vol. 71, No. 6, pp. 2011–2038. https://doi.org/10.1785/BSSA0710062011
23. Kouskouna, V., Kaperdas, V. and Sakellariou, N., (2020). "Comparing Calibration Coefficients Constrained from Early to Recent Macroseismic and Instrumental Earthquake Data in Greece and Applied to Eighteenth Century Earthquakes", *Journal of Seismology*, Vol. 24, pp. 293-317. https://doi.org/10.1007/s10950-019-09874-7
24. Martin, S. and Szeliga, W. (2010). "A Catalog of Felt Intensity Data for 570 Earthquakes in India from 1636 to 2009", *Bull. Seism. Soc. Am., Vol.* 100, No. 2, pp: 562–569. https://doi.org/10.1785/0120080328
25. Musson, R.M.W. (1996). "Determination of Parameters for Historical British Earthquakes", *Annals of Geophysics,* Vol. 39, pp. 1041–1048. DOI: https://doi.org/10.4401/ag-4035
26. Musson, R.M.W. (2005). "Intensity Attenuation in the UK", *J. Seismol.*, Vol. 9, pp. 73–86. https://doi.org/10.1007/s10950-005-2979-4
27. Musson, R.M.W., Grünthal, G. and Stucchi, M. (2010). "The Comparison of Macroseismic Intensity Scales", *J. Seismol.* Vol. 14, pp. 413–428. https://doi.org/10.1007/s10950-009-9172-0
28. Prajapati, S.K., Kumar, A., Chopra, S. and Bansal, B.K. (2013). "Intensity Map of Mw 6.9 2011 Sikkim–Nepal Border Earthquake and its Relationships with PGA: Distance and Magnitude", *Nat Hazards*, Vol. 69, pp. 1781–1801. https://doi.org/10.1007/s11069-013-0776-x
29. Szeliga, W., Hough, S., Martin, S. and Bilham, R. (2010). "Intensity, Magnitude, Location and Attenuation in India for Felt Earthquakes Since 1762", *Bull. Seism. Soc. Am.,* Vol. 100, pp. 570-584. https://doi.org/10.1785/0120080329